

# Pressure as a probe of the physics of $^{18}\text{O}$ -substituted $\text{SrTiO}_3$

E. L. Venturini and G. A. Samara

*Sandia National Labs, Albuquerque, New Mexico 87185, USA*

M. Itoh and R. Wang

*Tokyo Institute of Technology, Yokohama 226-8503, Japan*

(Received 24 July 2003; published 26 May 2004)

Studies of the dielectric properties and phase behavior of an  $^{18}\text{O}$ -substituted  $\text{SrTiO}_3$  (>97%  $^{18}\text{O}$ ), or STO-18, crystal at 1 bar and as functions of hydrostatic pressure and applied dc biasing electric field have shed much light on the mechanism of the  $^{18}\text{O}$ -induced ferroelectric transition in this material. Dielectric measurements reveal an equilibrium phase transition ( $T_c \approx 24$  K at 1 bar) and an enhancement of the static dielectric constant  $\epsilon'$  over that of normal (i.e.,  $^{16}\text{O}$ )  $\text{SrTiO}_3$ , or STO-16, over a large temperature range above  $T_c$ . This enhancement is quantitatively shown to be attributed to additional softening of the ferroelectric soft-mode frequency ( $\omega_s$ ) of STO-16, in agreement with lattice dynamic calculations. Thus, in STO-18, two effects due to the heavier mass of  $^{18}\text{O}$  conspire to induce the transition: (i) this additional softening of  $\omega_s$  and (ii) damping of quantum fluctuations. Pressure lowers  $T_c$  at the large initial rate of 20 K/kbar and completely suppresses the ferroelectric state leading to a quantum paraelectric state at  $\geq 0.7$  kbar, confirming earlier results. Very large effects of a biasing dc electric fields on the peak temperature and  $\epsilon'$  are also observed in the quantum regime reflecting the small characteristic energies of the system. The results also reveal a dielectric relaxation process near 10 K with interesting properties. The implications of all the results on our understanding of the physics of STO-18 are discussed.

DOI: 10.1103/PhysRevB.69.184105

PACS number(s): 67.70.+n, 77.22.Gm, 77.80.Bh

## I. INTRODUCTION

Isotopic substitution in ferroelectric (FE) crystals is known to produce significant changes in properties and has often led to a better understanding of the physics. This is particularly true of hydrogen-bonded ferroelectrics and antiferroelectrics where the substitution of deuterons for protons leads to very large effects due to the large mass difference between the two isotopes. The properties and physics of these hydrogen-bonded materials are well documented and generally understood.<sup>1-3</sup> There has also been increased recognition that there are significant effects and manifestations of the role of isotopic substitution in other classes of ferroelectrics. Hidaka<sup>4</sup> studied the isotope effect on the transition temperatures ( $T_c$ ) of a number of ferroelectrics and antiferroelectrics exhibiting both displacive and order-disorder transitions, but the effects are generally small.

A significant advance has been the recent discovery by Itoh *et al.*<sup>5</sup> that the substitution of  $^{18}\text{O}$  for  $^{16}\text{O}$  in  $\text{SrTiO}_3$  induces ferroelectricity in this material with a FE transition temperature  $T_c \approx 24$  K for the fully substituted  $^{18}\text{O}$  crystal.  $\text{SrTiO}_3$  (with naturally occurring  $^{16}\text{O}$ ) is a classic incipient ferroelectric; its soft-FE-mode frequency decreases with decreasing temperature ( $T$ ), but is stabilized at the lowest temperatures by quantum fluctuations. Consequently, the crystal does not undergo a FE transition and retains its tetragonal paraelectric (PE) structure down to the lowest temperatures. However, because of the delicate balance between the quantum fluctuations and the dipolar interactions, small perturbations can induce FE order as was demonstrated quite some time ago by the application of electrical bias,<sup>6</sup> uniaxial stress,<sup>7</sup> chemical substitution,<sup>8</sup> and now by  $^{18}\text{O}$  substitution.<sup>5</sup> Convincing evidence for the ferroelectricity of  $\text{SrTi}$

$(^{16}\text{O}_{1-x}^{18}\text{O}_x)_3$  for  $x \geq 0.33$  has come from dielectric, hysteresis loop, Raman, and birefringence measurements.<sup>5,9,10</sup> It is found that the FE transition temperature follows the expression<sup>11</sup>  $T_c = A(x - x_c)^{1/2}$ , predicted for quantum ferroelectrics,<sup>12,13</sup> where  $A = 30.4$  K and  $x_c = 0.33$ .

Because the occurrence of FE transitions in the quantum regime is determined by a very delicate balance between competing interactions, the application of hydrostatic pressure can be expected to strongly influence  $T_c$  and the dielectric properties and provide important insight into the physics. Indeed, this expectation has been shown to be the case for many ferroelectrics,<sup>3,13</sup> and it motivated the recent pressure studies of Wang *et al.*<sup>14</sup> of the dielectric properties of fully  $^{18}\text{O}$ -substituted  $\text{SrTiO}_3$ . Results were obtained on a  $(100)_c$ -oriented sample [i.e., field perpendicular to the  $(100)$  face referenced to the cubic ( $c$ ) phase], but the authors expressed two main concerns about their experiment.<sup>14,15</sup> The first has to do with the fact that pressure was generated in a so-called “clamped” high-pressure cell using the organic fluid fluorinert as the pressure-transmitting medium. In this cell, pressure is generated by pushing a piston into a die at room temperature, clamping the piston in place by a bolt, and then transferring the cell to a cryostat for low-temperature measurements. During cooling, the pressure changes due to differences in the thermal contraction of the cell and fluorinert, and, perhaps more seriously, the fluorinert ultimately freezes into a rigid glasslike solid at low temperatures, generating nonuniform (i.e., nonhydrostatic) stresses that could influence the results. The second concern is the use of a  $(100)_c$ -oriented crystal. On cooling cubic  $\text{SrTiO}_3$  undergoes an antiferrodistortive transition at 105 K at 1 bar into a tetragonal phase. This transition breaks up a monodomain  $(100)_c$ -oriented single crystal into a multidomain

sample. The concern is whether or not the multidomain nature of the sample influences the pressure response.

The present work was undertaken to address the above concerns as well as to more fully investigate the pressure dependence of the dielectric properties and to study the interplay between pressure and dc biasing electric fields on the FE transition and dielectric response. A specific goal of this work is to shed some light on the mechanism of the transition in the  $^{18}\text{O}$ -substituted material. Earlier experimental results interpreted the transition as due either to the percolation of FE microregions (FMRs) attributed to the presence of oxygen vacancies<sup>9</sup> or due to the formation of a low- $T$  domain state.<sup>16</sup> In this paper results on an  $^{18}\text{O}$ -substituted ( $>97\%$   $^{18}\text{O}$ ) crystal as well as on  $\text{SrTiO}_3$  ( $^{16}\text{O}$ ) were obtained and contrasted, revealing new insights into the physics of the substituted crystal.

## II. EXPERIMENTAL DETAILS

The measurements were made on  $(110)_c$ -oriented  $\text{SrTiO}_3$  ( $^{16}\text{O}$ ) and  $\text{SrTiO}_3$  ( $97\%$   $^{18}\text{O}$ ) crystals from the same material used by Itoh and co-workers.<sup>14,15</sup> In this orientation, the sample is cut with faces parallel to the  $(110)_c$  twin-boundary plane, resulting in a single domain in the tetragonal phase. For brevity these samples will henceforth be referred to as STO-16 and STO-18, respectively. The samples were thin rectangular plates ( $15.6\text{ mm}^2$  in area  $\times$   $0.37\text{ mm}$  thick) with polished and parallel faces. The electrical contacts on the large faces were of strongly adhering gold prepared from gold paste heated at  $873\text{ K}$  to burn the organic constituents.<sup>5,14</sup> The isotopic exchange method has been described by Itoh and co-workers,<sup>5,11</sup> and the  $^{18}\text{O}$  content was determined from the weight increment. For the present sample the  $^{18}\text{O}$  content exceeded  $97\%$  with  $T_c = 24\text{ K}$  at  $1\text{ bar}$ .

The pressure apparatus used helium (He) as the pressure-transmitting medium. Compressed helium is fed into the pressure cell through high-pressure tubing. He condenses and freezes at high pressure, but solid He is a very weak solid, allowing the maintenance of hydrostatic conditions. The real ( $\epsilon'$ ) and imaginary [ $\epsilon''$  ( $= \epsilon' \tan \delta$ )] components of the dielectric permittivity were measured as functions of temperature ( $4\text{--}292\text{ K}$ ), hydrostatic pressure ( $0\text{--}6\text{ kbar}$ ), frequency ( $10^2\text{--}10^6\text{ Hz}$ ), and dc biasing field ( $0\text{--}2000\text{ V/cm}$ ). The driving ac field amplitude was kept low ( $<1\text{ V/cm}$ ) to minimize nonlinearities in the dielectric response. Temperature measurements were carried out at a slow drift of  $\sim 0.2\text{--}0.5\text{ K/min}$ .

## III. RESULTS AND DISCUSSION

### A. Influence of pressure on the dielectric response

Figure 1 shows the temperature dependences of  $\epsilon'$  and  $\tan \delta$  at  $1\text{ bar}$  at  $10^4\text{ Hz}$  on both heating and cooling for STO-18. Results on STO-16 are shown for comparison. The STO-18  $\epsilon'(T)$  results exhibit a peak ( $T_c$ ) at  $24\text{ K}$  associated with the FE transition. Interesting features are the higher value of  $\epsilon'$  at the peak ( $\epsilon'_{\text{max}}$ ) on cooling and the thermal hysteresis in  $\epsilon'$  in the low- $T$  FE phase. As shown, the data at

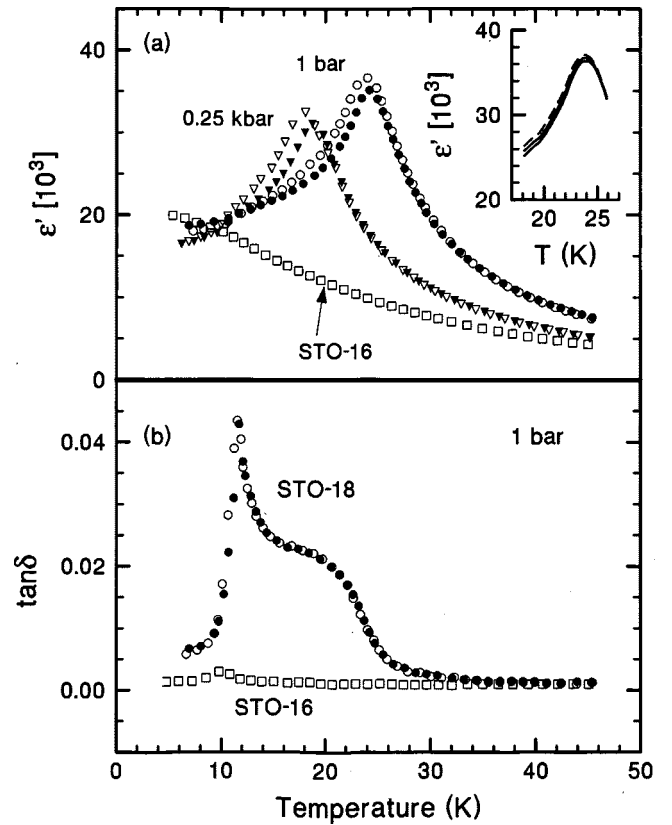


FIG. 1. Temperature dependences at  $1\text{ bar}$  and  $10^4\text{ Hz}$  of the dielectric constant  $\epsilon'$  and dielectric loss  $\tan \delta$  for our STO-18 ( $\geq 97\%$   $^{18}\text{O}$ ) crystal compared with similar results for an unsubstituted STO-16 crystal.  $\epsilon'(T)$  results for STO-18 at  $0.25\text{ kbar}$  are also shown to emphasize the observed thermal hysteresis in  $T_c$  and in the ferroelectric phase (solid symbols=heating; open symbols=cooling). The inset shows that the  $\epsilon'(T)$  response is essentially independent of frequency in the range  $10^2\text{--}10^5\text{ Hz}$ .

$1\text{ bar}$  in Fig. 1(a) reveal an unexpected  $\sim 0.2\text{ K}$  hysteresis in the high- $T$  PE phase. We believe that this is an artifact (not seen in scans under pressure) reflecting a thermal gradient between the sample and the Au +  $0.07\%$  Fe/Chromel thermocouple at ambient pressure. Correcting for this  $T$  offset by shifting the heating curve down by  $0.1\text{ K}$  and the cooling curve up by the same amount, there remains a small hysteresis of  $\sim 0.2\text{ K}$  in the  $T_c$ . Thermal hysteresis in  $T_c$  and in  $\epsilon'(T)$  in the FE phase are the usual signature of a thermodynamically first-order phase transition. We should hasten to mention, however, that very recent  $1\text{ bar}$  measurements by Dec *et al.*<sup>17(a)</sup> on a STO-18 crystal with  $94\%$   $^{18}\text{O}$  do not show a hysteresis in  $T_c$ , but do exhibit a higher  $\epsilon'_{\text{max}}$  on cooling than on heating as well as hysteresis in  $\epsilon'$  in the FE phase—features they attribute to a domain state below  $T_c$ . Going back to Fig. 1(a), we note that our high-pressure ( $0.25\text{ kbar}$ ) data reveal that the above-mentioned thermometry artifact above  $T_c$  is no longer present (perhaps compressed helium reduces the thermal gradients) and there is a more definite ( $\sim 1\text{ K}$ ) hysteresis in  $T_c$ . Thus the issue of the thermodynamic order of the transition at  $1\text{ bar}$  for the present crystal remains somewhat open.

A first-order phase transition for STO-18 has been predicted on the basis of an electron-phonon interaction lattice dynamical model.<sup>17(b)</sup> This model includes lattice anharmonicity as well as the important directional Ti-O  $p$ - $d$  hybridization via a nonlinear shell-model representation. Specifically, calculations using this model reveal, for the fully substituted crystal, small discontinuity at  $T_c$  in the temperature dependence of the core-shell displacement coordinate, which is analogous to an order parameter for the transition.

In these regards an interesting question is, what is the experimental signature of a first-order phase transition in the quantum regime? At high temperatures, first-order phase transitions in ferroelectrics are accompanied by measurable discontinuities at  $T_c$  in macroscopic properties such as the dielectric susceptibility (or  $\epsilon'$ ) and the polarization, in addition to thermal hysteresis in  $T_c$ . Are such discontinuities measurable in the quantum regime? We suspect that the answer is usually no for two general reasons. First, as  $T$  approaches 0 K, the free energy difference between the phases becomes relatively small, and, second, quantum fluctuations smear out the transition. The latter effect explains why  $\epsilon'(T)$  peaks at FE transitions in the quantum regime are always rounded.<sup>13</sup>

The results in the inset in Fig. 1(a) show that the  $\epsilon'(T)$  response is essentially frequency independent. The very weak dispersion in  $\epsilon'_{\text{max}}$  and in  $\epsilon'(T)$  in the FE phase, seen also by Itoh *et al.*,<sup>5</sup> is not uncommon in ferroelectrics and does not represent relaxor FE behavior, as will be discussed later. The rounded  $\epsilon'(T)$  peak is largely a manifestation of quantum fluctuations at low  $T$ , as already noted.

Figure 1(b) shows the  $\tan \delta(T)$  responses at 1 bar for both the STO-18 and STO-16 crystals at  $10^4$  Hz. The shoulder below  $\sim 25$  K in the STO-18 data is associated with the FE transition. It is followed by a large peak at  $\sim 10$  K. The  $\tan \delta$  peak is also seen, but at a much reduced amplitude in STO-16, as shown. These features, which were also observed by Wang and Itoh<sup>11</sup> in 1 bar data, appear to be associated with an unknown impurity or defect, and they do not influence the FE transition. They do, however, exhibit interesting and revealing effects that will be discussed in Sec. III E.

Figure 2 shows the influence of pressure of the  $\epsilon'(T)$  cooling response. First, we note the large shift of the transition to lower temperatures. The initial slope is  $dT_c/dP \cong -20$  K/kbar, a large effect. Second, there is a large decrease in the amplitude of the peak with pressure. At 0.70 kbar the transition is completely suppressed, and the  $\epsilon'(T)$  response closely resembles that of STO-16 at 1 bar shown in Fig. 1(a). These pressure effects are characteristic of displacive FE's in the quantum regime and can be understood in terms of soft-mode theory,<sup>3</sup> as we shall discuss below.

The inset in Fig. 2 shows the temperature-pressure phase diagram for STO-18. The data show clear evidence that  $T_c$  vanishes with an infinite slope—i.e.,  $dT_c/dP \rightarrow -\infty$  as  $T_c \rightarrow 0$  K. This is a requirement of the third law of thermodynamics for both first- and second-order phase transitions and establishes the equilibrium nature of the transition (as contrasted with relaxors) in STO-18.<sup>13</sup> The solid line in the inset is a fit of the  $T_c(P)$  data to the equation

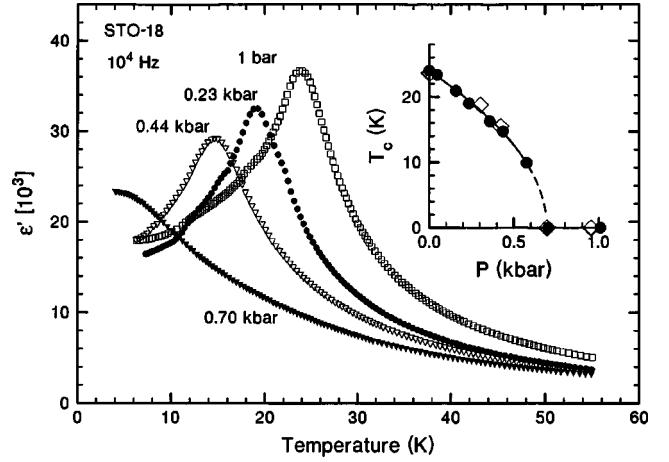


FIG. 2. The large influence of pressure on the  $\epsilon'(T)$  response leading to the complete suppression of the ferroelectric state. The inset shows the shift of  $T_c$  with pressure where the solid circles are our data and the open diamonds are from Ref. 14.

$$T_c = A(1 - P/P_c)^{1/2}, \quad (1)$$

with  $A = 23.9$  K and  $P_c = 0.69$  kbar. The form of this equation is predicted from theory for quantum ferroelectrics.<sup>11-13</sup> It is seen that the observed response obeys this expression quite well, again emphasizing the normal ferroelectric nature of STO-18.

At this point, it is important to note that, although there are some quantitative differences in the  $\epsilon'(T)$  at pressure between the results in Fig. 2 and those reported by Wang *et al.*<sup>14</sup> the general features of the responses are similar. In particular, the  $T_c(P)$  results of Wang *et al.*<sup>14</sup> obtained in the clamped pressure cell and shown by open diamonds in the inset in Fig. 2 are in close agreement with the present data. Thus the fluorinert pressure-transmitting medium used by Wang *et al.* has no significant influence on  $T_c(P)$ , and additionally, the results are not appreciably influenced by the multidomain nature of the initially (100)<sub>c</sub>-oriented sample used by Wang *et al.*

## B. Temperature and pressure dependences of the susceptibility in the high-temperature phase: The FE soft-mode response

Figure 3 shows  $\epsilon'(T)$  and  $1/\epsilon'(T)$  plots at 1 bar for both STO-18 and STO-16 over an extended temperature range. It is seen that  $\epsilon'$  for STO-18 is larger over the whole  $T$  range. For soft-mode ferroelectrics  $\epsilon'(T)$  in the PE phase is determined by the  $T$  dependence of the soft-mode frequency  $\omega_s$ , because the two quantities are connected by a Lyddane-Sachs-Teller relationship such that  $\omega_s^2 \epsilon' = \text{const}$ . This relationship is well established for STO-16, and we confirm it in Fig. 4 where we have plotted  $\omega_s^2$  and  $A/\epsilon'$  vs  $T$ . The solid diamonds are based on the average of three sets of  $\omega_s(T)$  data obtained on STO-16 from inelastic neutron scattering<sup>18</sup> and hyper-Raman measurements.<sup>19,20</sup> The dashed line is  $A/\epsilon'(T)$  using our STO-16  $\epsilon'(T)$  data and the equation  $\omega_s^2 \epsilon' = 2.48 \times 10^6 \text{ cm}^{-2}$ , where the constant was determined from the measured values of  $\omega_s$  and  $\epsilon'$  at 200 K. It is seen

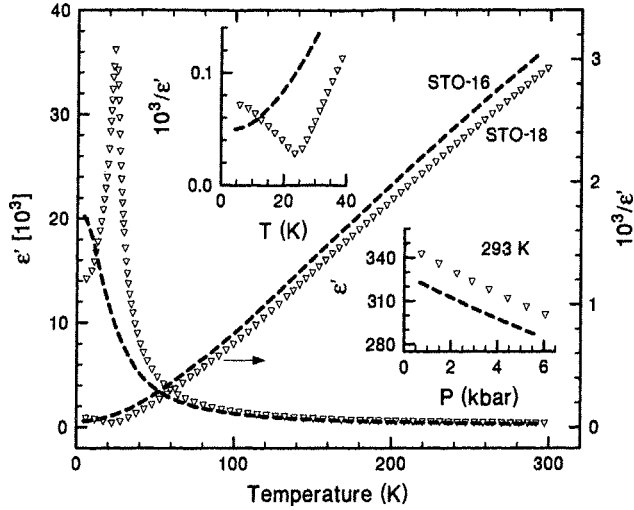


FIG. 3. Plots of  $\epsilon'(T)$  and  $1/\epsilon'(T)$  for STO-18 and STO-16 over an extended temperature range. The insets show an expanded view of the  $1/\epsilon'$  response near  $T_c$  and of the pressure dependences of  $\epsilon'$  at 293 K.

that the diamonds follow the dashed line quite accurately, confirming the above relationship.

The  $T$  dependence of  $\omega_s$  has not been reported for STO-18, but judging from the  $\epsilon'(T)$  data in Fig. 3, it should be very similar to that of STO-16 above  $\sim 60$  K. Thus, if we assume that the same constant ( $2.48 \times 10^6 \text{ cm}^{-2}$ ) applies to STO-18, we can use the present  $\epsilon'(T)$  data to calculate  $\omega_s(T)$ . The results, expressed as  $\omega_s^2(T)$ , are given by the solid line in Fig. 4. The slightly lower values of  $\omega_s$  at any given  $T$  for STO-18 compared to STO-16 reflects the expected softening of  $\omega_s$  on  $^{18}\text{O}$  substitution (see below). This is, of course, also seen in a somewhat higher  $\epsilon'$  for STO-18 above 60 K as shown in Fig. 3. The upper inset in Fig. 4 shows expanded  $\omega_s^2(T)$  plots in the region of the phase tran-

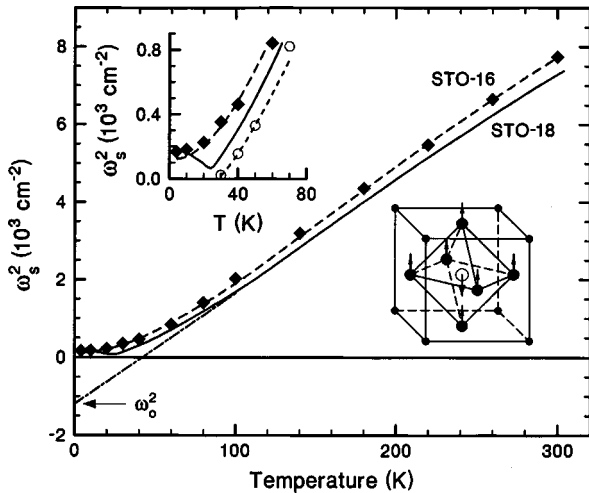


FIG. 4. Temperature dependences of the square of the soft-mode frequency,  $\omega_s^2$ , for STO-16 and STO-18 (see text for details). The insets show an expanded view of the behavior near  $T_c$  and a depiction of the eigenvector of the soft (Slater) mode.

sition in STO-18. The theoretical calculations of Bussmann-Holder *et al.*<sup>17(b)</sup> show qualitatively very similar results, but with a lower  $T_c$  of 15 K.

In a recent private communication<sup>21</sup> we have learned that the  $T$  dependence of  $\omega_s$  of STO-18 has been measured by both inelastic neutron scattering and hyper-Raman scattering. The resolution of the neutron data was not sufficient to resolve differences between STO-18 and STO-16, but the hyper-Raman data clearly reveal the additional softening of  $\omega_s$  of STO-18 compared to STO-16. The measured STO-18 data are shown (open circles) in the upper inset in Fig. 4. They parallel the solid line based on our  $\epsilon'(T)$  data, but are displaced to higher temperatures with an indicated  $T_c$  of 30 K, or 6–7 K above the actual  $T_c$  (suggesting perhaps an uncertainty in temperature measurement). Shifting the Raman-based data 6–7 K lower brings them close to our results. An additional hyper-Raman datum point was measured at 300 K, yielding  $\omega_s = 87 \text{ cm}^{-1}$ . This point is in good agreement with  $\omega_s^2(T)$  deduced from our  $\epsilon'(T)$  data in Fig. 4.

The FE soft mode in  $\text{SrTiO}_3$ , a long-wavelength transverse optic phonon, consists primarily of vibrations of the  $\text{Ti}^{4+}$  ions against their surrounding oxygen octahedra. The eigenvector of this mode (the Slater mode) is shown in the inset in Fig. 4. Clearly replacing  $^{16}\text{O}$  by  $^{18}\text{O}$  should reduce the frequency of this mode. Specifically, the ratio of the frequencies is related to the ratio of the effective masses ( $\mu$ ) of the Ti-O<sub>6</sub> octahedral units by

$$\omega_{18}/\omega_{16} = (\mu_{16}/\mu_{18})^{1/2}. \quad (2)$$

For the Slater mode it is readily shown that  $\omega_{18}/\omega_{16} = 0.97$ —i.e., a 3% decrease in  $\omega_s$  on complete  $^{18}\text{O}$  substitution in  $\text{SrTiO}_3$ .<sup>22</sup> Our dielectric data accurately confirm this prediction. This is most clearly seen in the inset in Fig. 3, where  $\epsilon'$  is plotted versus pressure at 293 K and the  $\epsilon'$  curve for STO-18 is 6% higher than the STO-16 curve. Specifically at 1 bar,  $\epsilon'_{18} = 348$  and  $\epsilon'_{16} = 328$  so that  $\epsilon'_{18}/\epsilon'_{16} = 1.06$ —i.e., a 6% enhancement, which, from  $\epsilon' \propto (1/\omega_s^2)$ , implies a 3% decrease in  $\omega_s$ , as calculated.

Going back to Fig. 4, we see that  $\omega_s^2(T)$  for STO-18 parallels that for STO-16 above  $\sim 60$  K, but deviates as shown and, as expected, on approaching  $T_c$ . It is this additional softening which triggers the FE transition, making it difficult for the disordering tendency of quantum fluctuations to overcome the ordering tendency of the dipolar interactions.

The observed decrease of  $T_c$  of STO-18 and the ultimate complete suppression of the FE phase with pressure can be understood in terms of soft-mode theory as has been demonstrated for other displacive ferroelectrics.<sup>3</sup> Inherent in the soft-mode concept for FE transitions is the premise that the crystal is unstable in the harmonic approximation with respect to the soft mode.<sup>3</sup> Specifically, the square of the harmonic frequency,  $\omega_0^2$ , is presumed to be sufficiently negative (i.e.,  $\omega_0$  is imaginary) that this mode cannot be stabilized by zero-point fluctuations alone. Thermal fluctuations then renormalize  $\omega_0$  and make it real at finite temperatures,

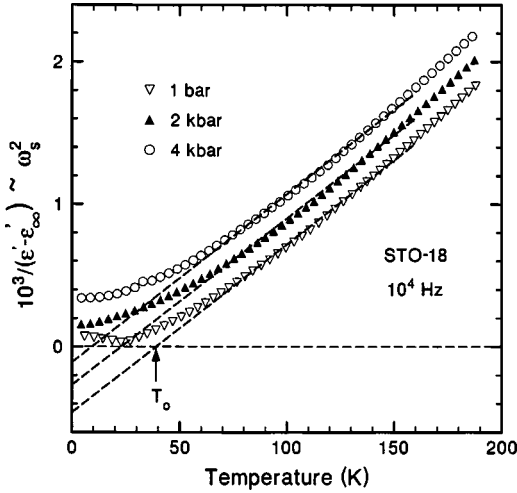


FIG. 5. Plots of  $\omega_s^2(T)$  or  $1/\epsilon'(T)$  at different pressures for STO-18.

thereby stabilizing the lattice. Formally, the renormalized frequency of mode  $j$  with wave vector  $q$  for an anharmonic crystal can be written as<sup>3,23</sup>

$$\omega_T^2(jq) = \omega_0^2(jq) + \sum_{\mu k} g_{j\mu}^{(4)}(qk)x \frac{1}{2\omega(\mu k)} \coth \frac{\omega(\mu k)}{2k_B T}, \quad (3)$$

where  $g_{j\mu}$  are effective fourth-order coupling constants and the summation is over all modes  $\mu$  and wave vectors  $k$ . At suitably high temperatures, thermal fluctuations are dominant, and the second term on the right-hand side of Eq. (3) is linear in  $T$  as confirmed by the data above  $\sim 60$  K (Fig. 4).

Extrapolation of this linear response to  $T=0$  K yields as a measure of  $\omega_0^2$  a negative value—i.e., an imaginary harmonic mode frequency. The deviation from linear  $\omega_s^2(T)$  below  $\sim 60$  K is attributed to quantum fluctuations and is predicted from Eq. (3). One consequence of quantum fluctuations in ferroelectrics is to suppress  $T_c$  below its classical limit  $T_c^{\text{cl}}$  [the intersection of the linear  $\omega_s^2(T)$  line with the  $T$  axis in Fig. 4].<sup>13</sup> Evidence for this suppression for STO-18 is seen in Fig. 4 where the actual  $T_c$  [minimum in  $\omega_s^2(T)$ ] falls well below  $T_c^{\text{cl}}$ .

According to soft-mode theory,  $\omega_0^2$ , which is determined by the overcancellation of the short-range forces by the long-range Coulomb forces, should become less negative and, ultimately, positive with increasing pressure, making  $\omega_s$  real and finite and thereby the crystal stable at all temperatures: i.e., the transition vanishes. This is what we observe, as demonstrated in Fig. 5 where we have plotted  $10^3/\epsilon'$  (which is proportional to  $\omega_0^2$ ) vs  $T$  at different pressures. These results are quite revealing. The intersections of the linear high- $T$  (classical) response with the  $x$  and  $y$  axes yield the Curie-Weiss temperature ( $T_0$ ) and  $\omega_0^2$ , respectively. The results in Fig. 5 show that (i)  $T_0$  decreases with pressure with a slope  $dT_0/dP = -7.5$  K/kbar, which is comparable to that of many perovskite ferroelectrics in the classic regime,<sup>3</sup> and (ii)  $\omega_0^2$  should become positive (and thus the classic transition should vanish) at  $\sim 5$  kbar. The facts that  $dT_c/dP$  for

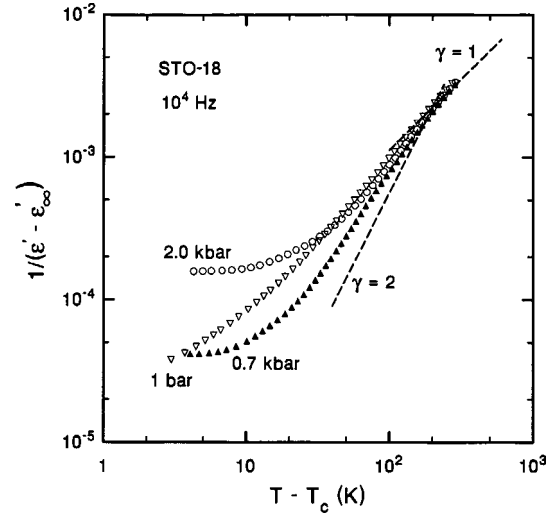


FIG. 6. Log-log plots of  $(\epsilon' - \epsilon_\infty)$  vs  $(T - T_c)$  for STO-18 at different pressures.

STO-18 is much larger ( $-20$  K/kbar) and the actual transition vanishes at 0.69 kbar (and not at  $\sim 5$  kbar) are clear manifestations of the role of quantum fluctuations in this system.

One of the consequences of the suppression of the phase transition is the presence of a special critical point: namely,  $T_c = 0$  K.<sup>12,13</sup> This point, which is referred to as the quantum displacive limit, is characterized by special critical exponents. Its presence gives rise to classical-to-quantum crossover phenomena. Quantum suppression and the response at and near this limit,  $T_c = 0$  K, have been studied extensively on the basis of lattice dynamic models solved within the framework of both classical and quantum statistical mechanics.<sup>12</sup> One specific prediction from these models is that the critical exponent  $\gamma_T$  of the generalized susceptibility equation

$$\epsilon' = \epsilon'_\infty = C(T - T_c)^{\gamma_T}, \quad (4)$$

which is  $\gamma_T = 1$  in the high- $T$  classical regime, should reach a value  $\gamma_T = 2.0$  at the displacive limit. Figure 6 is a log-log plot of our  $\epsilon'(T)$  results on STO-18. The expectation from theory is that in the quantum regime  $\gamma_T = 2$  at  $\sim 0.7$  kbar (where  $T_c \approx 0$  K), after which  $\gamma_T$  should decrease. The results in Fig. 6 qualitatively show the expected behavior; however,  $\gamma_T$  is significantly  $< 2$  at 0.70 kbar.

Wang and Itoh<sup>11</sup> studied the behavior of  $\gamma_T$  as a function of  $^{18}\text{O}$  composition at 1 bar. They observed an increase in  $\gamma_T$  on approaching the quantum displacive limit ( $T_c = 0$  K at 33%  $^{18}\text{O}$ ) from both the high- and low-concentration regimes with the suggestion that a value of  $\gamma_T = 2.0$  may be reached. The theory also predicts that  $T_c(P)$  should obey Eq. (1) as  $T_c \rightarrow 0$  K. This is indeed observed, as we discussed earlier.

Another manifestation of the suppression of the transition is the formation of quantum paraelectric (QPE) state—a state characterized by a large, temperature-independent  $\epsilon'$  over a relatively large temperature range at low  $T$ 's. Such a state obtains for STO-16 at 1 bar and for STO-18 at  $P \geq 0.7$  kbar

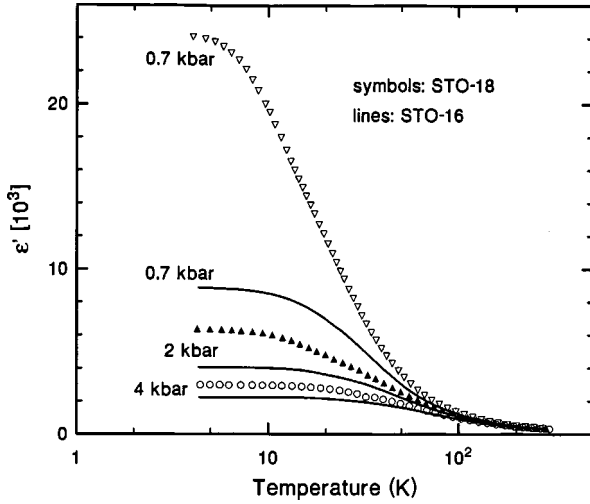


FIG. 7. Temperature dependence of  $\epsilon'$  in the quantum paraelectric phases of STO-18 and STO-16 at different pressures.

and as shown in Fig. 7. The quantum PE state extends to higher  $T$  with increasing pressure as shown for both STO-16 and STO-18. Qualitatively similar results were observed by Wang *et al.*<sup>14</sup> The  $T$  dependence of  $\epsilon'$  in this regime is often described in terms of the Barrett equation, as recently done<sup>14</sup> for STO-18. It is also well described in terms of Eq. (3).

### C. Influence of dc biasing fields

It is well established that dc biasing fields have a strong influence on the properties of ferroelectrics, especially in the quantum regime where the characteristic energies are small. This was demonstrated by Itoh *et al.*<sup>5</sup> for (100)<sub>c</sub>-oriented STO-18 crystal at 1 bar and is shown in Fig. 8 for our (110)<sub>c</sub>-oriented sample. The large suppression of the peak amplitude  $\epsilon'_{\max}$  and the shift of the peak temperature ( $T_m$ ) to higher temperatures are the expected behaviors for quantum ferroelectrics and can be understood as follows. The application of a biasing field stabilizes the local potential of a dipole

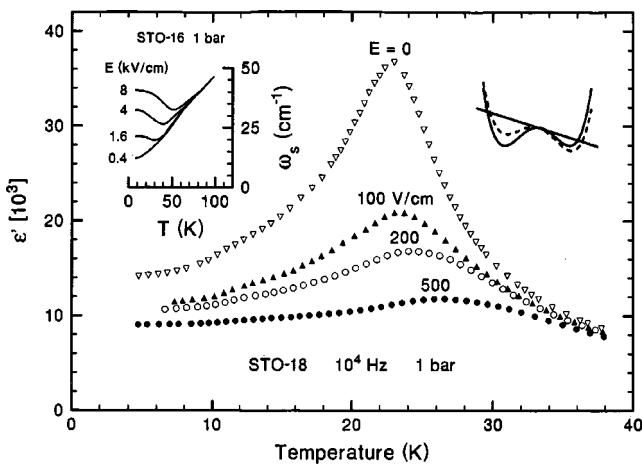


FIG. 8. Bias electric field dependence of the  $\epsilon'(T)$  response of STO-18 at 1 bar. The insets show the influence of bias on the potential for dipolar reorientation (right) and on  $\omega_s(T)$  for STO-16 (left) from Ref. 24.

lar entity, making one of its potential minima deeper and the other shallower (inset in Fig. 8). Thus more thermal energy is needed to overcome the deeper barrier, leading to a higher  $T_m$ . Additionally, the field stiffens the soft mode and aligns and clamps the polarization of the sample, reducing its small signal ac susceptibility—i.e., suppressing  $\epsilon'$ . These effects are well known from Landau free energy theory,<sup>2</sup> which predicts that  $T_m$  increases with field strength as  $E^{2/3}$ . The results in Fig. 8 show the expected increase of  $T_m$  with  $E$ , but they do not extend over sufficient ranges of  $E$  and  $T_m$  to provide a quantitative test. Another feature to note is the fact that these very large biasing field effects with modest biasing fields occur only in the quantum regime. They vanish above  $\sim 40$  K as shown in Fig. 8.

It should be noted here that it has long been known<sup>24</sup> that a dc biasing field stiffens  $\omega_s$  of STO-16 and that sufficiently high bias breaks the tetragonal symmetry and induces ferroelectricity with a broad  $\epsilon'(T)$  peak. The FE transition is reflected in a broad minimum in  $\omega_s(T)$  as shown in the inset in Fig. 8. This minimum shifts to higher  $T$ 's with increasing field. Thus these results qualitatively mimic the behavior of STO-18 in Fig. 8; however, the fields to induce the large changes seen for STO-18 are much smaller than those required for STO-16. Specifically, while, for STO-16,  $dT_m/dE = 1.9$  K cm/kV,  $dT_m/dE = 7$  K cm/kV for STO-18—a reflection of the fact that both  $\omega_s$  and quantum fluctuations are smaller for STO-18.

### D. Nature of the phase transition in STO-18

Much of the evidence from the present as well as earlier work by Itoh *et al.*<sup>5</sup> has indicated that highly substituted STO-18 exhibits on cooling a transition to a normal FE state at  $\sim 24$  K at 1 bar. From a thermodynamic point of view, the vanishing of  $T_c$  with an infinite slope  $dT_c/dx$  at a critical concentration<sup>11</sup> or at a critical pressure (Fig. 2) is indicative of an equilibrium phase transition. The evidence also points to the softening of the FE mode in the high- $T$  paraelectric phase with increasing  $^{18}\text{O}$  substitution as the trigger for the transition. In STO-16 this mode also softens with decreasing  $T$ , but ultimately quantum fluctuations prevent it from softening sufficiently to induce the transition. In STO-18 two effects due to the heavier mass of  $^{18}\text{O}$  conspire to induce the transition: (i) additional softening of the FE mode in the tetragonal phase and (ii) damping of the quantum fluctuations at low  $T$ 's. And it is only in the low- $T$  quantum regime where the characteristic energies of the system are so small that the  $\sim 12\%$  change in mass produced by  $^{18}\text{O}$  substitution can produce such large effects. Thus, e.g.,  $^{18}\text{O}$  substitution in  $\text{BaTiO}_3$  raises its FE transition temperature (393 K) by only  $\sim 0.9$  K.<sup>4</sup>

Despite the above evidence for a displacive soft mode nature for the transition, there have been a number of puzzling and unresolved observations. Raman scattering studies on an 87%  $^{18}\text{O}$ -substituted crystal by Kasahara *et al.*<sup>9</sup> revealed a 20% softening of the  $A_{2u}$ -type zone-center optic mode below  $T_c$ , but did not find the  $E_u$  soft FE mode which was expected to drive the transition in the low- $T$  phase. Normally, the symmetry of this phase would be expected to be

orthorhombic, and thus the Raman results are not consistent with such symmetry. However, recent second-harmonic generating (SHG) results on STO-18 have shed some light on this point.<sup>25</sup> While the rapid rise of the SHG signal below  $T_c$  confirms a sharp transition to a polar state, analysis of the SHG signal suggests the existence of locally variant mixtures of eight triclinic polar domains. These domains transform into a single orthorhombic domain under a sufficiently large  $E$  field perpendicular to the tetragonal  $c$  axis of the high- $T$  phase.<sup>25</sup> This complex mixture of domains and the interplay between different symmetries would make the observation of a distinct soft mode in the FE phase with Raman scattering difficult. As for the behavior above  $T_c$ , our results in Fig. 4 and the lattice dynamical calculations<sup>17</sup> and the very recent hyper-Raman data<sup>21</sup> leave no doubt about the soft-mode nature of the transition, as already discussed.

The Raman study<sup>9</sup> also suggested that ferroelectric microregions similar to those believed to exist in undoped  $\text{KTaO}_3$  (Ref. 26) are present in STO-18. These FMR's are attributed to the presence of oxygen vacancies ( $V_{\text{O}}$ 's) introduced by the high-temperature (1273 K) processing required to achieve  $^{18}\text{O}$  for  $^{16}\text{O}$  substitution in  $\text{SrTiO}_3$ .<sup>5</sup> Each  $V_{\text{O}}$  produces a dipolar entity, which polarizes a nanoregion or microregion around it, forming a FMR. This finding led the authors<sup>9</sup> to suggest that the mechanism for the transition in STO-18 is percolation of the FMR's as they grow with decreasing  $T$  in a manner analogous to that observed in dilute Ca-doped  $\text{SrTiO}_3$  (Refs. 27 and 28) and Nb-doped  $\text{KTaO}_3$  (Ref. 13). Analysis of the Raman data provided the change in the size ( $R_o$ ) of the FMR's with  $T$ ,<sup>9</sup> and the suggestion is made that the phase transition occurs when  $R_o$  becomes larger than the separation between oxygen vacancies. The present results, including the absence of significant frequency dispersion in  $\epsilon'(T)$  (inset, Fig. 1), argue against such a mechanism for the transition in the present crystal.

Such a mechanism, if valid, would raise a number of questions. While  $V_{\text{O}}$  would induce a dipole, which would form a FMR in the highly polarizable  $\text{SrTiO}_3$  host, it is doubtful that there would be sufficient number of  $V_{\text{O}}$ 's to induce the transition. (We are not aware of a value for the  $V_{\text{O}}$  formation energy in  $\text{SrTiO}_3$ , but it must be on the order of several volts.) A second point is that  $V_{\text{O}}$  hopping is unlikely to occur at temperatures approaching  $T_c$  of STO-18, so that the  $V_{\text{O}}$  must be immobile, or frozen, as is the case for  $\text{KTaO}_3$ ,<sup>29</sup> making it difficult for the polarization of the vacancy produced FMR's to follow the oscillations in the ac driving field. Without such fluctuations in the polarization, which would require  $V_{\text{O}}$  hopping, it is difficult to explain the buildup of the susceptibility (or  $\epsilon'$ ) as  $T$  approaches  $T_c$  from above.

Other observations have led to the suggestion that the low- $T$  phase of STO-18 is a *domain state*.<sup>16</sup> These observations include a nonlinear dielectric response reflected in a strong dependence of  $\epsilon'$  on the amplitude of the ac driving field at  $T$ 's  $\ll T_c$  and decrease in the magnitude of the remanent polarization with time at  $T$ 's slightly below  $T_c$ . Nonlinear dielectric responses have been observed in both oxide and hydrogen-bonded FE's and are usually attributed to the dynamics of different domain structures below  $T_c$ .<sup>30,31</sup> The

fact that the observed nonlinearity in STO-18 is observed at much lower ac field amplitudes than in other FE's is most likely related to the much smaller characteristic energy scale of STO-18 in the quantum regime. This small energy scale could also be responsible for the observed decrease of the remanent polarization with time.

The concept of a low- $T$  domain state was proposed quite some time ago by Imry and Ma<sup>32</sup> and Aharony.<sup>33</sup> Their theoretical results showed that when the order parameter has continuous symmetry, the ordered state of a large system of less than  $d=4$  dimensions is unstable against an arbitrarily weak random field (RF)—i.e., a field much weaker than the interactions that favor the ordered state. Instead of a long-range ordered state, it becomes energetically more favorable for such a system to break up on cooling into “sufficiently large” domains to form a low- $T$  domain state. The size of the domain is determined by a balance between the domain wall energy and the statistics of the RF.

As for STO-18, the question then is what is the nature of the low- $T$  state and not the mechanism for the transition. As noted earlier, there is compelling evidence that the low- $T$  phase is ferroelectric, but is the order long range as in a normal ferroelectric or is it broken up by the frozen RF's (presumably associated with  $V_{\text{O}}$ 's) that lead to a domain state? In reality, in the absence of a dc biasing field, all normal ferroelectrics are made up of randomly oriented domains. So it is the size of the domains that distinguishes a normal FE state from a domain state. It is the higher degree of statistical fluctuations when the domains are very small that changes the dynamics and contributes to the nonlinear response of  $\epsilon'(T)$  to ac fields. In contrast to normal FE domain walls, the RF-induced domain walls are subject to RF pinning which leads to relaxation in the dielectric response.<sup>34</sup>

### E. The 10-K relaxation

The dielectric loss peak at  $\sim 10$  K seen in Fig. 1(b) has been observed in other STO-18 samples.<sup>11,35,36</sup> It exhibits some remarkable pressure-induced changes which we now discuss. Figure 9 is a summary of some of the results. First, we note that the  $\tan \delta$  peak associated with the FE transition (which due to its proximity to the 10-K peak appears as a shoulder at  $\sim 20$  K) shifts to lower  $T$  with pressure and merges into the 10-K peak by  $\sim 0.5$  kbar (not shown). We also note that, whereas there is no frequency dispersion in the location of the  $\tan \delta(T)$  shoulder associated with the FE transition, the 10-K  $\tan \delta$  peak exhibits the frequency dispersion of a relaxor. The relaxational frequency follows Arrhenius kinetics as shown by the inset in Fig. 9 with  $E = 14$  meV and  $\omega_o = 7 \times 10^{10}$  Hz. Within the scatter of the data, both the peak temperature and dispersion appear to be independent of pressure over the small pressure range covered. This is significant when contrasted with the large shift of  $T_c$  as will be discussed below. However, the amplitude of the  $\tan \delta$  peak exhibits the strong and revealing pressure dependence shown, where we show only data at  $10^4$  Hz. Other frequencies show qualitatively similar results. It is seen that the amplitude decreases monotonically in the FE phase, but then drops precipitously (by almost an order of magnitude)

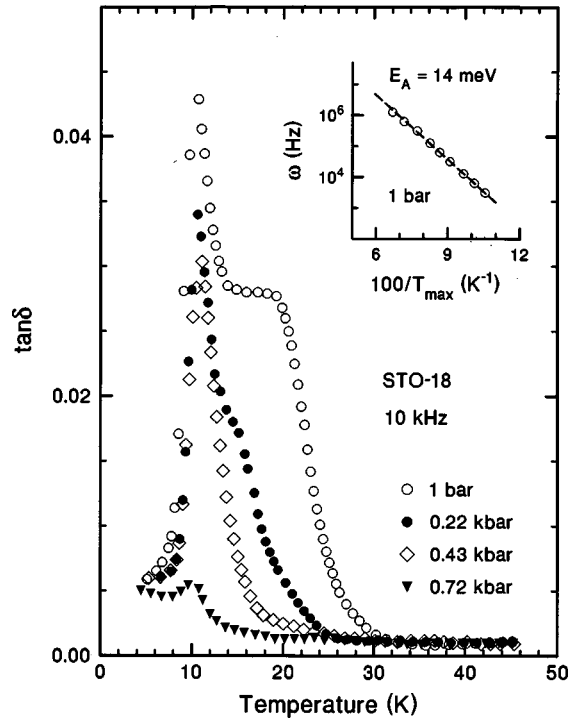


FIG. 9. The influence of pressure on the dielectric loss  $\tan \delta$  of STO-18 measured at different frequencies with emphasis on the 10-K relaxation peak.

when  $T_c$  vanishes and the sample crosses over to the QPE state at  $\geq 0.7$  kbar. In the QPE state the amplitude of  $\tan \delta$  is quite small and decreases only slightly with pressure.

The 10-K relaxational peak also occurs in STO-16 and has been studied at 1 bar (Refs. 35 and 37). Our results on this crystal agree with these earlier studies. Interestingly, the amplitude of this peak in STO-16 is comparable to that in STO-18 in its QPE phase [cf. Figs. 1(b) and 9, 0.72 kbar]. Viana *et al.*<sup>37</sup> found that the kinetics of this relaxation in STO-16 at 1 bar obeys an Arrhenius law above  $\sim 9$  K with  $E = 13.8$  meV and  $\omega_o = 6.3 \times 10^{10}$  Hz, parameters that are essentially the same as we find for both STO-18 and STO-16. The kinetics takes on a non-Arrhenius character at lower temperatures.<sup>37</sup> The authors interpreted this relaxation to be characteristic of a quantum phase transition into a coherent quantum state, but suggested that alternative explanations could be given in terms of ferroelectric microdomains and the relaxation of a well-defined defect state. Our results and those of Wang and Itoh<sup>35</sup> strongly favor the latter interpretation.

Wang and Itoh<sup>35</sup> found  $E = 13.8$  meV for STO-16 at 1 bar for data between  $\sim 9.5$  and 12 K and observed that  $E$  decreases somewhat with  $^{18}\text{O}$  substitution. Within experimental uncertainty, we do not see any difference in  $E$  between our STO-16 and STO-18 crystals. In a more recent study, Kleemann<sup>38</sup> find  $E = 11.4$  K for an  $^{18}\text{O}$ -substituted crystal with no systematic deviation from Arrhenius behavior between 5 and 14 K. There are some differences in the 1 bar values of  $E$  and  $\omega_o$  among the reported values. Scatter in the data may account for some of these differences, but it is not clear that this can explain all.

The fact that the 10-K relaxation occurs in STO-16 along with the results in Fig. 9 suggests that it is native to STO and is not associated with the high-temperature process used to exchange  $^{16}\text{O}$  by  $^{18}\text{O}$ . The results in Fig. 9 are indicative of strong coupling between this relaxation and the polarization in the FE phase, a coupling that strongly enhances the amplitude of  $\tan \delta$ . This coupling is lost on loss of polarization in STO-18 as  $T_c \rightarrow 0$  K and the sample becomes a QPE.

A number of questions remain. What is the nature of the defect responsible for the 10-K relaxation and why does it not shift with pressure, given the large pressure dependences of  $T_c$  and the dielectric properties? Clearly, the defect has an associated orientable dipole moment leading to the observed relaxational loss peak. It is tempting to speculate that this relaxation is akin to that observed even the purest in  $\text{KTaO}_3$  samples at  $\sim 40$  K (Ref. 39) and which has the same amplitude of  $\tan \delta$  as that for STO-16 or for STO-18 in its QPE state—i.e., at  $\geq 0.7$  kbar. The  $\text{KTaO}_3$  relaxation has been attributed to an unknown impurity or defect, and, significantly, it exhibits Arrhenius kinetics with  $E = 38$  meV and  $\omega_o = 1 \times 10^{11}$  Hz, both quantities quite comparable to those seen in our STO-18 crystal given the difference in peak temperatures.

As for the absence of detectable shift in the 10-K peak temperature with pressure at the 1-kbar level, we believe that this is strong evidence that the peak is a normal dipolar lattice impurity or defect whose impurity potential and motional dynamics are determined by normal lattice properties and have nothing to do with the soft FE mode that determines  $T_c$  and its extremely large pressure dependence. For normal lattice properties pressures on the order of 1 kbar are relatively minor perturbations, and one needs to go to considerable higher pressure to observe measurable changes in crystal potentials. Explanations of the 10-K relaxation in terms of FE microclusters and quantum phase transitions can be ruled out as these would exhibit large pressure effects in the quantum regime where the characteristic energies are small.<sup>13</sup> We believe that it is simply due to an unknown impurity or defect, a conclusion that is shared by others.<sup>35,38</sup> We have extended study of this relaxational phenomenon under both pressure and field bias to Ca-doped STO-16. A more detailed account of the results on this material and on STO-16 and STO-18 will be published elsewhere.

#### IV. CONCLUDING REMARKS

Analysis of our dielectric data has demonstrated quantitatively the additional softening of the soft-mode frequency ( $\omega_s$ ) of  $\text{SrTiO}_3$  caused by the substitution of  $^{18}\text{O}$  for  $^{16}\text{O}$ . The fully substituted  $^{18}\text{O}$  crystal exhibits primarily a displacive equilibrium transition to a low-temperature ferroelectric state. Because the transition occurs at low temperatures ( $T_c = 24$  K at 1 bar), two effects due to the heavier mass of  $^{18}\text{O}$  undoubtedly conspire to induce the transition: the additional softening  $\omega_s$  and the damping of the quantum fluctuations that suppress the expected displacive transition in the unsubstituted  $\text{SrTiO}_3$ . Our results suggest that the phase transition at 1 bar maybe thermodynamically first order in



agreement with theoretical results from an anharmonic coupled electron-phonon model;<sup>17(b)</sup> however, new dielectric results<sup>17(a)</sup> on a different crystal (94%  $^{18}\text{O}$ ) did not reveal significant thermal hysteresis in  $T_c$ , suggesting that the order of the transition may deserve further examination on other crystals.

The occurrence of the ferroelectric transition in STO-18 is determined by a balance between competing short- and long-range interactions, and pressure is an excellent variable for delicately tuning this balance and ultimately suppressing the transition. The unusually large effects of pressure and electrical bias on the dielectric properties and  $T_c$  of STO-18 are a reflection of the fact that the transition occurs in the quantum regime where the characteristic energies are so small,

allowing small applied fields to cause very large changes in properties.

#### ACKNOWLEDGMENTS

The authors express their appreciation to David Lang for technical support in performing the dielectric measurements. We are very thankful to Professor W. Kleemann for his thorough review of and valuable comments on the manuscript. The work at Sandia National Laboratories was supported by the Division of Materials Sciences and Engineering, Office of Basic Energy Sciences, U.S. Department of Energy. Sandia is a multiprogram laboratory operated by Sandia Corporation, a Lockheed Martin Company, for the U.S. Department of Energy under Contract No. DE-AC04-94AL85000.

- 
- <sup>1</sup>R. Blinc and B. Zeks, *Soft Modes in Ferroelectrics and Antiferroelectrics* (American Elsevier, New York, 1974).
- <sup>2</sup>M. E. Lines and A. M. Glass, *Principles and Applications of Ferroelectrics and Related Materials* (Clarendon, Oxford, 1977).
- <sup>3</sup>G. A. Samara and P. S. Peercy, in *Solid State Physics*, edited by H. Ehrenreich, R. Spaepen, and D. Turnbull (Academic, New York, 1981), Vol. 36, p. 1, and references therein.
- <sup>4</sup>T. Hidaka, *Ferroelectrics* **137**, 291 (1992).
- <sup>5</sup>M. Itoh, R. Wang, Y. Inaguma, T. Yamaguchi, Y.-J. Shan, and T. Nakamura, *Phys. Rev. Lett.* **82**, 3540 (1999).
- <sup>6</sup>P. A. Fleury, J. F. Scott, and J. M. Worlock, *Phys. Rev. Lett.* **21**, 16 (1968).
- <sup>7</sup>H. Uwe and T. Sakudo, *Phys. Rev. B* **13**, 271 (1976).
- <sup>8</sup>J. G. Bednorz and K. A. Müller, *Phys. Rev. Lett.* **52**, 2289 (1984).
- <sup>9</sup>M. Kasahara, H. Hasebe, R. Wang, M. Itoh, and Y. Yagi, *J. Phys. Soc. Jpn.* **70**, 648 (2001).
- <sup>10</sup>K. Yamanaka, R. Wang, M. Itoh, and K. Ito, *J. Phys. Soc. Jpn.* **70**, 3213 (2001).
- <sup>11</sup>R. Wang and M. Itoh, *Phys. Rev. B* **64**, 174104-1 (2001).
- <sup>12</sup>T. Schneider, H. Beck, and E. Stoll, *Phys. Rev. B* **13**, 1123 (1976); R. Morf, T. Schneider, and E. Stoll, *ibid.* **16**, 462 (1977), and references therein.
- <sup>13</sup>G. A. Samara, in *Solid State Physics*, edited by H. Ehrenreich and F. Spaepen (Academic, New York, 2001), Vol. 56, pp. 239–483, and references therein.
- <sup>14</sup>R. Wang, N. Sakamoto, and M. Itoh, *Phys. Rev. B* **62**, R3577 (2000). See also R. Wang and M. Itoh, in *Perovskite Materials*, edited by K. Peoppelmeier, A. Navrotsky, and R. Wentzcovitch, *Mater. Res. Soc. Symp. Proc.* 718 (Materials Research Society, Pittsburgh, PA, 2002), pp. 251-256.
- <sup>15</sup>M. Itoh (private communication).
- <sup>16</sup>R. Wang and M. Itoh, *Phys. Rev. B* **62**, R731 (2000).
- <sup>17</sup>(a) J. Dec, W. Kleemann, and M. Itoh, in *Proceedings of the NATO Advanced Workshop on Disordered Ferroelectrics [Ferroelectrics (to be published)]*; (b) A. Bussmann-Holder, H. Büttner, and A. R. Bishop, *J. Phys.: Condens. Matter* **12**, L115 (2000).
- <sup>18</sup>Y. Yamada and G. Shirane, *J. Phys. Soc. Jpn.* **26**, 396 (1969).
- <sup>19</sup>K. Inoue, N. Asai, and T. Sameshima, *J. Phys. Soc. Jpn.* **50**, 1291 (1981).
- <sup>20</sup>A. Yamanaka, M. Kataoka, Y. Inaba, K. Inoue, B. Hehlen, and E. Courtens, *Europhys. Lett.* **50**, 688 (2000).
- <sup>21</sup>Y. Minaki, M. Kopyayashi, Y. Tsujimi, T. Yagi, M. Nakanishi, R. P. Wang, and M. Itoh, *J. Korean Phys. Soc.* **42**, Supplement S, S1290–S1293 (2003).
- <sup>22</sup>M. Itoh and R. Wang, *Appl. Phys. Lett.* **76**, 221 (2000).
- <sup>23</sup>R. A. Cowley, *Philos. Mag.* **11**, 673 (1965); *Adv. Phys.* **12**, 421 (1963).
- <sup>24</sup>J. M. Worlock and P. A. Fleury, *Phys. Rev. Lett.* **19**, 1176 (1967).
- <sup>25</sup>L. Zhang, W. Kleemann, R. Wang, and M. Itoh, *Appl. Phys. Lett.* **81**, 3022 (2002).
- <sup>26</sup>H. Uwe, K. B. Lyons, H. L. Carter, and P. A. Fleury, *Phys. Rev. B* **33**, 6436 (1986).
- <sup>27</sup>U. Bianchi, J. Dec, W. Kleemann, and J. G. Bednorz, *Phys. Rev. B* **51**, 8737 (1995).
- <sup>28</sup>E. L. Venturini, G. A. Samara, and W. Kleemann (unpublished).
- <sup>29</sup>K. Leung, *Phys. Rev. B* **63**, 134415-1-11 (2001).
- <sup>30</sup>See, e.g., S. Li, W. Cao, and L. E. Cross, *J. Appl. Phys.* **69**, 7219 (1991).
- <sup>31</sup>See, e.g., Q. Tan and D. Viehland, *Phys. Rev. B* **53**, 103 (1996); *J. Appl. Phys.* **81**, 361 (1997).
- <sup>32</sup>Y. Imry and S. Ma, *Phys. Rev. Lett.* **35**, 1399 (1975).
- <sup>33</sup>A. Aharony, *Solid State Commun.* **28**, 667 (1978).
- <sup>34</sup>W. Kleemann, J. Dec, R. Wang, and M. Itoh, in *Fundamental Physics of Ferroelectrics 2003*, edited by P. K. Davies and D. J. Singh, *AIP Conf. Proc. No. 677* (AIP, Melville, NY, 2003), pp. 26–32.
- <sup>35</sup>R. Wang and M. Itoh, *Ferroelectrics* **262**, 125 (2001).
- <sup>36</sup>L. Zhang, W. Kleemann, J. Dec, R. Wang, and M. Itoh, *Eur. Phys. J. B* **28**, 163 (2002).
- <sup>37</sup>R. Viana, P. Lunkenheimer, J. Hemberger, R. Böhmer, and A. Loidl, *Phys. Rev. B* **50**, 601 (1994).
- <sup>38</sup>W. Kleemann (private communication).
- <sup>39</sup>B. Salce, J. L. Graviil, and L. A. Boatner, *J. Phys.: Condens. Matter* **6**, 4077 (1994), and references therein.